

Transmembrane and Juxtamembrane Structure of α L Integrin in Bicelles

Wahyu Surya¹*, Yan Li¹, Oscar Millet², Tammo Diercks², Jaume Torres^{1*}

1 School of Biological Sciences, Nanyang Technological University, Singapore, Singapore, **2** Structural Biology Unit, CIC BioGUNE, Derio Vizcaya, Spain

Abstract

The accepted model for the interaction of α and β integrins in the transmembrane (TM) domain is based on the pair α IIb β 3. This involves the so-called outer and inner membrane association clasps (OMC and IMC, respectively). In the α chain, the OMC involves a GxxxG-like motif, whereas in the IMC a conserved juxtamembrane GFFKR motif experiences a backbone reversal that partially fills the void generated by TM separation towards the cytoplasmic half. However, the GFFKR motif of several α integrin cytoplasmic tails in non-bicelle environments has been shown to adopt an α -helical structure that is not membrane-embedded and which was shown to bind a variety of cytoplasmic proteins. Thus it is not known if a membrane-embedded backbone reversal is a conserved structural feature in α integrins. We have studied the system α L β 2 because of its importance in leukocytes, where integrin deactivation is particularly important. Herein we show that the backbone reversal feature is not only present in α Lb but also in α L-TM when reconstituted in bicelles. Additionally, titration with β 2 TM showed eight residues clustering along one side of α L-TM, forming a plausible interacting face with β 2. The latter orientation is consistent with a previously predicted reported polar interaction between α L Ser-1071 and β 2 Thr-686.

Citation: Surya W, Li Y, Millet O, Diercks T, Torres J (2013) Transmembrane and Juxtamembrane Structure of α L Integrin in Bicelles. PLoS ONE 8(9): e74281. doi:10.1371/journal.pone.0074281

Editor: Edward F. Plow, Lerner Research Institute, United States of America

Received: April 12, 2013; **Accepted:** July 30, 2013; **Published:** September 12, 2013

Copyright: © 2013 Surya et al. This is an open-access article distributed under the terms of the Creative Commons Attribution License, which permits unrestricted use, distribution, and reproduction in any medium, provided the original author and source are credited.

Funding: This work has been funded by the National Research Foundation of Singapore (www.nrf.gov.sg) grant NRF-CRP4-2008-02 (J.T.). The funders had no role in study design, data collection and analysis, decision to publish, or preparation of the manuscript.

Competing Interests: The authors have declared that no competing interests exist.

* E-mail: jtorres@ntu.edu.sg

† These authors contributed equally to this work.

Introduction

Integrins are heterodimeric type I transmembrane (TM) proteins formed by non-covalent association of an α and a β subunit. In humans, 18 α -chains can interact with 8 different β -chains to form 24 different α/β heterodimers [1]. Each subunit contains a large extracellular domain, a single membrane-spanning α -helix and a short cytoplasmic tail [2]. By spanning the membrane, integrins serve as a dynamic linkage between cytoplasm and extracellular space, transducing signals across the membrane to mediate various functions [3]. Information transduction in integrins is bidirectional, inside-out or outside-in. Inside-out signaling involves separation of integrin cytoplasmic tails and TM domain, and subsequent ectodomain conformational changes, which alter the affinity of integrins for extracellular ligands [4–6]. Deletions or mutations that are expected to destabilize α/β association of TM or cytoplasmic domains in the α and β subunits, have been shown to activate integrins [7–9]. Conversely, inactivation is achieved by enhancing heterodimerization, e.g., using intermolecular disulfide bonds; in fact disulfide scanning of the α IIb β 3 TM region revealed the TM heterodimer interface [10].

Two models of heterodimeric α/β TM interaction were proposed based on electron microscopy and a computational approach showing different crossing angles for ‘resting’ and ‘activated’ states [5,11]. For the first model, interaction was mediated via a GxxxG-like motif located in both α and β TM chains. This proposed mode of interaction is reminiscent of that

found previously for the homodimer glycoporphin A (GpA) [12]. For the second proposed mode of interaction [11,13], the β helix is rotated by approximately 90° from its orientation in the GpA-like model. This latter model has been validated for α IIb β 3 using activating mutations at the transmembrane domain [14], cysteine cross-linking of the full integrin [10,15], and NMR studies of the α IIb β 3 transmembrane heterodimer structure in bicelles [16]. Thus, this is currently accepted to represent the interaction of the two TM domains of α IIb and β 3 in the resting state.

This accepted model has been further refined in the case of α IIb β 3 [15–17]. Specifically, the two TMs are in close proximity at the extracellular half of the membrane, forming an outer membrane association clasp (OMC) that involves the GxxxG-like motif in α IIb, Gly-972xxxGly-976, and Gly-708 in β 3. The TMs separate towards the cytoplasmic half, and the void is partially filled with an inner membrane association clasp (IMC), formed by a juxtamembrane backbone reversal in α IIb that participated by two phenylalanines, Phe-992 and Phe-993. The latter are part of a conserved α chain GFFKR motif. Lastly, a salt bridge between Arg-995 of α IIb and Asp-723 of β 3 has also been identified [16]. At present, no other detailed structural model for other integrin TMs is available.

In contrast to the above model for the juxtamembrane backbone reversal, the GFFKR motif in several α integrins e.g., in α IIb, α 1, α M, α L, α X or α 4 [18–24], formed an α -helical structure that was not membrane-embedded. However, most of these reports included the cytoplasmic tail without the TM domain, although in some cases they were myristoylated and

attached to detergent micelles. Other reports included the TM domain, but the structure was determined in the presence of organic solvents or in presence detergent micelles. Thus, it is possible that the failure to observe such reverse turn in the above examples was due either to the absence of the TM domain, or to the fact that detergent micelles or organic solvents do not provide the appropriate environment for such structural feature.

Several reports show binding of several cytosolic proteins to a region in the α chain that encompasses this conserved motif, e.g., serine-threonine phosphatase 2A (PP2A) [25], nischarin [26–28], calcium- and integrin- binding protein 1 (CIB1) [29–31], sharpin [32], or mammary-derived growth inhibitor (MDGI) [33]. Although the precise binding location of these proteins has not been elucidated, these data suggest that an α -helical solvent exposed structure is physiologically relevant.

Although the membrane-embedded reverse backbone has been observed in the presence of the TM domain and lipids, whether in bicelle systems or membranes [15,16], it has only been reported for α IIB integrin. Therefore, observing a membrane-embedded reverse turn in an α integrin-TM different from α IIB would support that this structural feature is conserved, and that it represents one of the possible conformations of the GFFKR motif in all integrins.

We have chosen to use the system α L β 2 because of its importance in leukocytes, where it is involved in adhesion, migration, cytotoxicity, proliferation, and antigen presentation [34]. The importance of the GFFKR motif in α L has been demonstrated by looking at the effect of deletion of this motif in a transgenic mouse, which led to a constitutive α L β 2-mediated cell adhesion [35]. Additionally, in these fast-migrating cells, integrin deactivation is particularly important, and we proposed previously that the latter could be facilitated by hydrogen bond interaction between TMs [36–38]. Thus, to elucidate if the reverse turn at the GFFKR motif is also found in α L when the peptide is reconstituted in bicelles, and to delineate the α L interfacial residues involved in α L/ β 2 interaction, we have expressed, purified and determined the structure of α L TM in bicelles by solution NMR. Further, titration experiments with non-labeled β 2 TM show which residues in α L are most affected by this interaction.

Experimental Procedures

Integrin α L TM and β 2 TM Expression and Purification

The DNA sequence encoding the TM region of human α L integrin, residues 1057–1103 (Fig. 1A), was cloned into a pET-28b expression vector, whereas the sequence for human TM β 2 integrin, residues 675–710, was cloned into pNIC28-Bsa4. G685F and G689F mutations at in the GxxxG-like region of β 2 TM were subsequently introduced by site-directed mutagenesis with the relevant pair of primers. All constructs were expressed with an N-terminal 6-His tag, cleavable by tobacco etch virus (TEV) protease.

The plasmids were transformed into *E. coli* strain BL21 codon-plus for protein expression. For expression of non-labeled peptides, the culture was grown in terrific broth (TB) media at 37°C until an OD₆₀₀ of 2. Protein expression was induced overnight at 25°C by adding 1 mM IPTG. The cells were harvested by centrifugation at 7500×g and stored at –80°C.

For expression of stable isotope-labeled peptides, the culture was initially grown in LB media at 37°C until an OD₆₀₀ of 0.7. The cells were collected and resuspended into M9 minimal media at 25% of the initial volume, to achieve a high-density culture as described previously [39,40]. The media was supplemented with ¹⁵N-NH₄Cl, ¹³C-glucose, ¹³C/²H-glucose, or D₂O (Cambridge

Isotope Laboratories), according to the desired labeling scheme: ¹⁵N-labeled, ¹⁵N/¹³C-labeled, and ¹⁵N/¹³C-labeled with partial (50%) and complete (99%) deuteration. Cultures were further grown for 1 h before inducing protein expression with 1 mM IPTG at 25°C overnight. Cells were harvested as mentioned above and stored at –80°C.

Cell pellets were resuspended in lysis buffer containing 20 mM Tris pH 8.0, 300 mM NaCl, 5 mM imidazole, 2 mM β -mercaptoethanol and 10% glycerol. Complete lysis was achieved by adding 1.5% Triton X-100, followed by sonication and microfluidization. The crude cell lysate was clarified by centrifugation at 40,000×g and applied onto pre-equilibrated Ni-NTA resin (Bio-Rad Profinity IMAC Ni²⁺-charged). The resin was washed with the 30 column volume (CV) of washing buffer A and 3 CV of washing buffer B. Washing buffer A consists of lysis buffer supplemented with 25 mM imidazole while washing buffer B consists of washing buffer A supplemented with 1.8 mM N-dodecyl- β -D-maltopyranoside (DDM). The bound peptide was cleaved on-column by adding TEV protease with 3 hours incubation period at room temperature. Cleaved peptide was collected, TCA-precipitated and lyophilized. The peptides were extracted by adding methanol to the lyophilized powder and removing the precipitates by centrifugation.

Peptide identity and purity was assessed by SDS-PAGE and MALDI-TOF MS (Fig. S1 in File S1). When deemed necessary, the peptides were further purified by using reversed-phase HPLC. Purification was achieved by applying isopropanol-acetonitrile (80/20 (v/v) with 0.1% TFA) linear gradient on a Phenomenex Jupiter C18 semipreparative column (250×10 mm, 300 Å pore size, 5 μ m particle size). The peptides were lyophilized and stored in –20°C.

NMR Sample Preparation

The phospholipid bicelle system was composed of 1,2-dimyristoyl-*sn*-glycero-3-phosphate (DMPC, Avanti Polar Lipids) and 1,2-dihexanoyl-*sn*-glycero-3-phosphate (DHPC, Avanti Polar Lipids). Peptide-DMPC mixture in methanol was dried under N₂ stream followed by high vacuum. DHPC solution in appropriate buffer was added into the dried peptide-DMPC mixture, vortexed and sonicated. In this way, lyophilized α L TM peptides were reconstituted into DHPC-DMPC bicelle (3% w/v, q=0.3) at 0.6 mM (corresponding to approximately 1:100 peptide-to-lipid ratio) buffered with 50 mM potassium phosphate at pH 6.5.

Partial alignment of the α L-TM/bicelle complexes relative to magnetic field was obtained by using compressed and stretched polyacrylamide hydrogels [41,42]. Axially symmetric alignment tensor coefficients (axiality and rhombicity) were calculated using MODULE [43]. Briefly, 250 μ L gels were co-polymerized with 0.6 mM α L TM-bicelle in 50 mM potassium phosphate at pH 6.5, from a 4.2% or 4.6% w/v solution of acrylamide, bis-acrylamide, and 2-acrylamido-2-methyl-1-propanesulfonate (AMPS) with acrylamide-bis ratio of 49:1 (w/w) and acrylamide-AMPS molar ratio of 94:6.

NMR Spectroscopy – NMR experiments were performed at 30°C using Bruker Avance-III 800 and Avance-II 700 NMR spectrometers with cryogenic probes. Sodium 2,2-dimethyl-2-silapentane-5-sulfonate (DSS) was used as the internal reference for ¹H nuclei. The chemical shifts of ¹³C and ¹⁵N nuclei were calculated from the ¹H chemical shifts. The NMR data were processed using TopSpin 3.1 (www.bruker-biospin.com) and analyzed using CARRA (www.nmr.ch). Sequence-specific assignment of backbone ¹H^N, ¹⁵N, ¹³C^o and ¹³C^o was achieved by using 2D [¹H-¹⁵N]-TROSY-HSQC, 3D TROSY-optimized HNCO, HNCA, HN(CO)CA, HN(CA)CB, and HN(COCA)CB experiments on a fully-deuter-

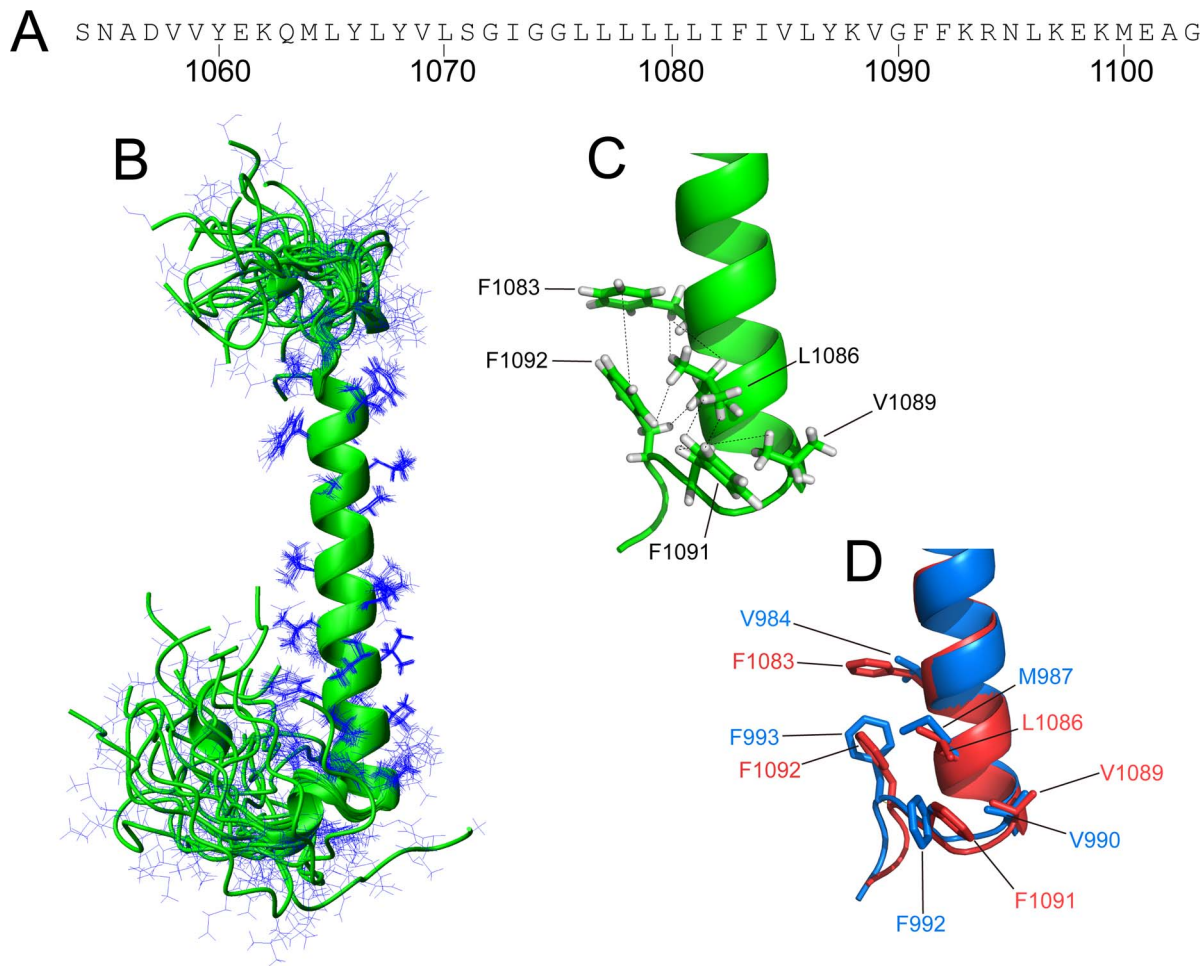


Figure 1. Structure of the integrin α L TM domain. (A) Sequence of the α L TM peptide used in this work with α L chain-context numbering; (B) superposition of an ensemble of 20 calculated simulated annealing structures of α L-TM; side-chains are shown as line representation; (C) α L close up of the IMC region with main residues involved in the formation of the reverse turn. For illustration, some NOEs found are represented as broken lines; (D) structural alignment of α L-TM (Leu-1078 to Arg-1094, in red), and α IIb-TM (PDB code: 2K1A, Leu-979 to Arg-995, in blue). The side-chains are shown as line representation and hydrogen atoms are omitted for simplicity.
 doi:10.1371/journal.pone.0074281.g001

ated $^{15}\text{N}/^{13}\text{C}$ -labeled α L TM. Side-chain resonances were assigned using 3D ^{15}N -resolved NOESY-HSQC (120 ms mixing time), (H)CCH-TOCSY and ^{13}C -resolved NOESY-HSQC (120 ms mixing time) on non-deuterated and partially-deuterated $^{15}\text{N}/^{13}\text{C}$ -labeled α L TM. To identify membrane-embedded residues, the NMR sample was lyophilized overnight and reconstituted in 99% D_2O . Immediately after reconstitution, 2D $[^1\text{H}-^{15}\text{N}]$ -TROSY-HSQC was collected. The spectra measuring $^1\text{H}-^{15}\text{N}$ heteronuclear steady-state NOE were acquired with and without a 3s period of proton saturation. Titration experiments were performed by adding increasing amounts of non-labeled β 2 TM to 50 μM ^{15}N -labeled α L TM until there were no further changes in the $[^1\text{H}-^{15}\text{N}]$ -HSQC spectra, from 1:0.5 to 1:6 α/β molar ratio.

Structure Calculation

NOE distance restraints to calculate the structures of α L TM domain were obtained from ^{15}N -NOESY-HSQC and ^{13}C -NOESY-HSQC spectra, respectively. Backbone dihedral angle restraints (ϕ and ψ) were derived from ^{13}C , $^{13}\text{C}^\alpha$, $^{13}\text{C}^\beta$, $^1\text{H}^\alpha$ and $^1\text{H}^\beta$ chemical shift values using TALOS [44]. The short-range and medium range NOE connectivities were used to establish the

sequence-specific ^1H NMR assignment and to identify elements of the regular secondary structure. Structure calculations were performed using CYANA 3.0 [45,46] and visualized using MOLMOL [47] and PyMOL (Delano Scientific). CNS 1.3 [48,49] was used to refine the structure using the standard simulated annealing protocol. A total of 20 structures have been calculated and the structure statistics are summarized in Table S1 in File S1. The structure of integrin α L TM domain has been deposited on the Protein Data Bank (PDB) with ID 2m3e, and the assigned chemical shifts have been deposited on the Biological Magnetic Resonance Bank (BMRB) with ID 18958.

Results

Structure of the α L TM Domain in Phospholipid Bicelles

The structure of bicelle-reconstituted integrin α L TM domain (α L) was determined by using a set of 2D and 3D NMR experiments on the $^{15}\text{N}/^{13}\text{C}$ -labeled peptide with varying deuteration levels. Upon reconstitution into DHPC-DMPC bicelles, α L forms a linear α -helix which extends approximately from Leu-1065 to Val-1089 (Fig. 1A–B and Fig. S2 in File SS). This α -helix comprises $\sim 50\%$ (25 residues) of the whole peptide.

This is significantly lower than ~ 80 – 90% α -helix estimated by FTIR when this peptide was reconstituted in lipid bilayers (Fig. S3A in File S1), but the value is comparable to $\sim 60\%$ (30 residues) estimated from CD when the peptide was reconstituted in bicelles (Fig. S3B in File S1).

The conserved GFFKR motif follows immediately the α -helix, with Phe-1091 and Phe-1092 reinserting into the bicelle (Fig. 1B–C) and forming a backbone reversal, only observed previously in α IIB in bicelles [16]. The structure is consistent with Phe-1091 making hydrophobic contacts to Leu-1086 and Val-1089, whereas the side-chain of Phe-1092 packs against Phe-1083 and Leu-1086, as indicated by NOE connectivities between these residues (Fig. 1C and Fig. 2). Thus Phe-1083, Leu-1086, Phe-1091 and Phe-1092 constitute a hydrophobic surface which potentially forms an interaction site with β 2-TM. The superposition of our α L-TM model and that reported for α IIB-TM shows high structural similarity between the two proteins (Fig. 1D). This strongly suggests that the backbone reversal of the GFF motif is a characteristic structural feature of α integrin subunits when reconstituted in bicelles. Alignment of the rest of the TM domains produced an α C RMSD of 0.83 Å. In comparison, the α C RMSD with a recently published α 1 TM structure in micelles for which no reverse turn was observed [24] was 1.3 Å.

The membrane-embedded region of α L was identified through an H^N - D_2O exchange experiment. From a comparison between $[^1H$ - $^{15}N]$ -TROSY-HSQC spectra in water and in 99% D_2O , amide protons of a stretch of 21 residues from Val-1069 to Val-1089, plus Phe-1092 in the GFFKR motif, are protected from exchange (Fig. 3A). This number is considerably lower than the 35 exchange-protected residues estimated from FTIR using the peptide reconstituted in lipid bilayers (see IR spectra before and after exchange in Fig. S3C in File S1).

The dynamic properties of α L were studied using a steady-state $[^1H$, $^{15}N]$ heteronuclear NOE experiment. The majority of the residues correspond to a well-folded structure, with the central

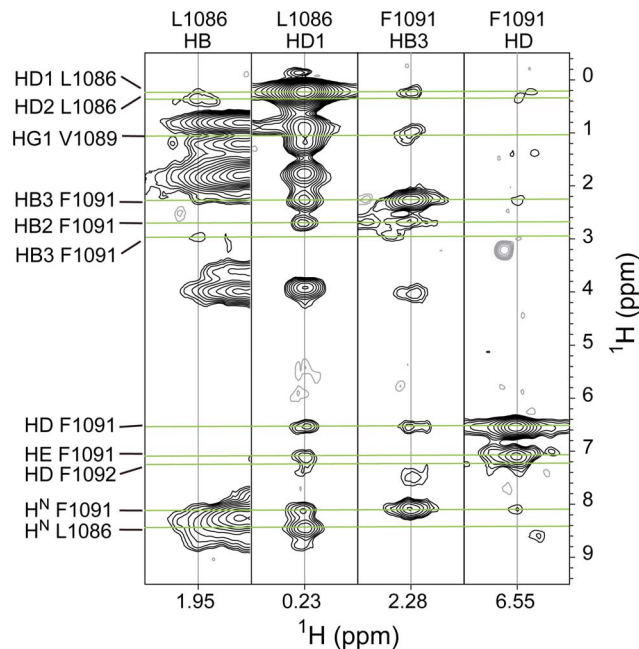


Figure 2. NOE connectivity in the IMC region of α L TM. Four selected strips from ^{15}N -NOESY-HSQC and ^{13}C -NOESY-HSQC show some NOE contacts among Leu-1086, Val-1089, Phe-1091, and Phe-1092. doi:10.1371/journal.pone.0074281.g002

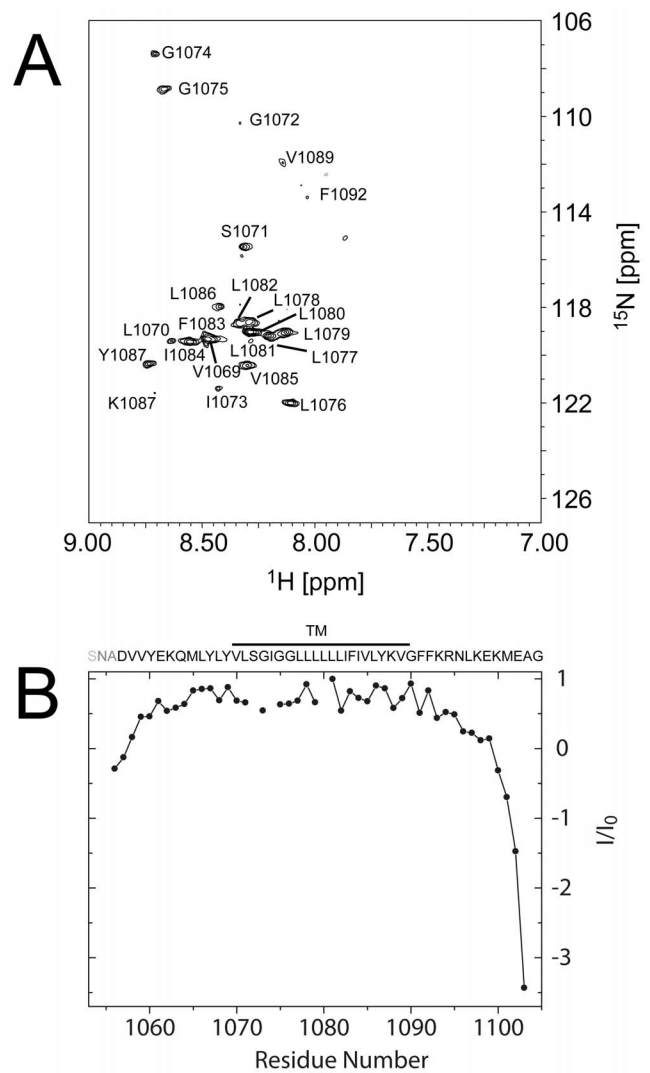


Figure 3. Integrin α L TM H^N - H_2O chemical exchange and backbone dynamics. (A) $[^1H$ - $^{15}N]$ -TROSY-HSQC spectra in 99% D_2O . The cross peaks are labeled by one-letter code and the residue number; (B) $[^1H$, $^{15}N]$ steady-state heteronuclear NOE experiment. The three extra N-terminal residues, SNA, are grayed out. The residues protected from H/D exchange are indicated by a line, and labeled as TM. doi:10.1371/journal.pone.0074281.g003

part, Val-1059 to Asn-1095, being the most stable (Fig. 3B). The backbone RMSD of the central TM region from a set of 20 conformers is 0.23 Å, indicating a well-defined structure. On the other hand, the N and C termini, especially the latter, are highly dynamic regions (see also Fig. 1B).

Interaction between the TMs of α L and β 2

To determine what residues in α L mediate interaction with β 2, we titrated unlabeled β 2 TM into ^{15}N -labeled α LTM, and monitored the changes in the $[^1H$ - $^{15}N]$ -HSQC spectra. Qualitative examination of the spectra at a 1:2 α L/ β 2 molar ratio revealed eight residues with pronounced intensity reduction upon addition of β 2 peptide, namely Leu-1067, Tyr-1068, Ser-1071, Gly-1072, Gly-1074, Gly-1075, Tyr-1087 and Phe-1091 (Fig. 4A). Met-1064 also showed intensity reduction, albeit less obvious, whereas Asn-1095 experienced a chemical shift change. Intensity of these resonances was reduced with increasing β 2 peptide, until

the signal disappeared (Fig. 4B). A summary of these changes for the α/β molar ratio 1:2 is shown in Fig. 4C. The same results were observed when the titration was performed with a β 2 TM mutant where the 'G' residues in the GxxxG-like motif were changed to Phe, i.e., G685F and G689F (data not shown). The latter confirms that β 2 does not interact with α L via its GxxxG-like motif, consistent with the reported α IIB/ β 3 model of interaction for resting integrins [10,16,50]. The affected residues cluster on one side of the α L-TM, with residues Ser-1071 and Gly-1075, located at positions 1 and 5 in the OMC region GxxxG-like motif, having the same orientation as the residues involved in the IMC (Fig. 5). At the same time, these locations are separated by a stretch on non interacting residues, consistent with the TM separation previously observed for the α IIB/ β 3 system (see above). Thus, the putative IMC and OMC regions of α L TM are oriented to form a plausible interacting face with β 2 TM.

The presence of $\alpha\beta$ heterodimerization in our titration is supported by comparison of the TROSY-HSQC spectrum of 0.1 mM α L with that of 0.6 mM concentration obtained in identical conditions shows that increasing α L concentration does not lead to intensity reduction of the peaks (Fig. S4 in File S1). Therefore, the peak intensity reduction observed in our titration

experiment is not caused by α L homodimerization. Also, membrane-mimicking screening studies [51] show a predominant presence of $\alpha\beta$ heterodimers in a 1:1 integrin $\alpha\beta$ -TM mixture at 0.1 mM, identical concentration to that used here, or even at 0.01 mM. In the latter report, in contrast, it was shown that homomeric species increase in DPC and SDS micelles, and also in organic solvents [51].

Discussion

Importance of Environment for Integrin TM Reconstitution

Phospholipid bicelles have been successfully used for structural determination of membrane proteins by solution NMR [52], especially with bicelles of low q-ratios. The inclusion of a small proportion of long-chain lipid makes this system more membrane-like than micelles, yet still reasonably small for solution NMR studies. The better suitability of bicelles, relative to micelles, has been demonstrated in the study of the integrin α IIB/ β 3 TM heterodimer in bicelles [16,51]; in micelles, these two TMs were not found to heterodimerize [51,53].

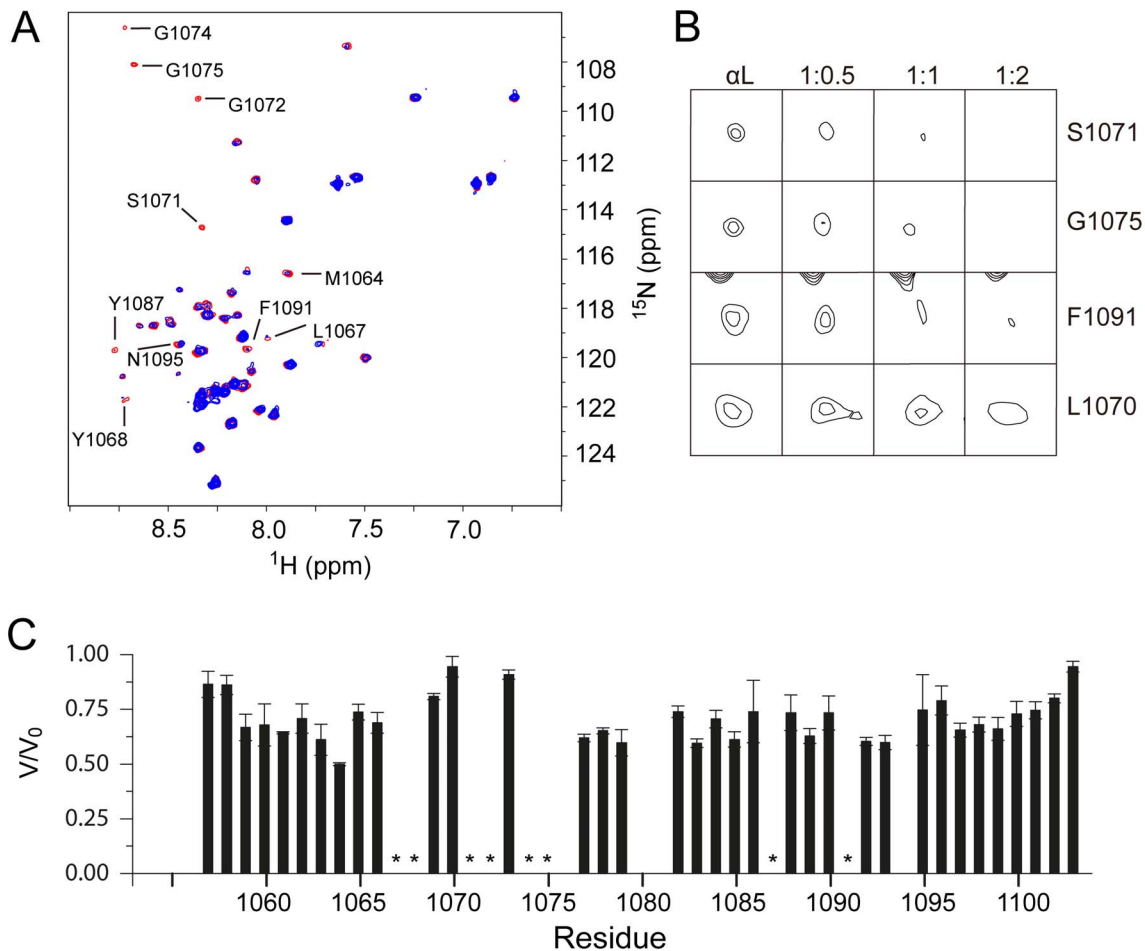


Figure 4. Interaction between α L and β 2 TM domains. (A) Result of the titration of ^{15}N -labeled α L TM by unlabeled β 2 TM at α L/ β 2 1:2 molar ratio, monitored by ^1H - ^{15}N HSQC. The spectra in red represent the α L TM alone, while the one in blue was obtained after addition of β 2 TM. Residues most affected are labeled; (B) Selected regions in the ^1H - ^{15}N HSQC spectrum at increasing α L/ β 2 molar ratios indicated showing intensity reduction and disappearance of selected peaks Ser-1071, Gly-1075, Phe-1091. Leu-1070 is shown for comparison; (C) Peak intensities expressed as ratio between peak volume after (V) and before (V_0) addition of unlabeled β 2 TM to labeled α L TM. Residues that experience extreme line broadening are indicated by *. Missing/overlapping resonances, e.g., R1094, are not shown. doi:10.1371/journal.pone.0074281.g004

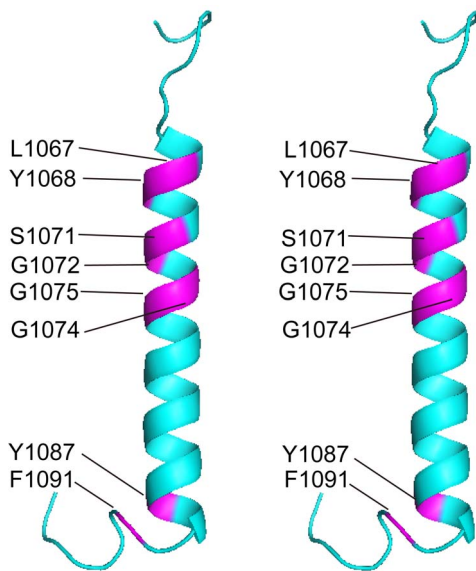


Figure 5. Putative interacting face of α L TM. Stereo view ribbon representation of the α L TM domain (Val-1058 to Lys-1097) with residues most affected by heterodimerization with β 2 shown in magenta.

doi:10.1371/journal.pone.0074281.g005

In addition, the unique backbone reversal for α Ib, was reported in bicelles [17] and full length integrin in biological membranes [15]. In presence of detergent micelles or organic solvents, the region encompassing the GFFKR motif adopted an α -helical conformation in α Ib and several other integrins [18–23,54], even when the TM domain was also present (e.g., [24,54]). Thus, not only the reconstitution environment may play a critical role for the observation of this reverse turn, but cytoplasmic peptide length and proper conformation of the TM region may be important. Indeed, the reverse turn formed by the GFFKR motif makes contacts with several side-chains in the α TM domain, as we (this paper) and others [16] have observed. Herein a hydrophobic packing is proposed in the α L-TM for the reinserted Phe-1091 and Phe-1092 against Phe-1083 and Leu-1086. The titration data also suggests that Phe-1091 is strongly involved in the interaction with β 2 TM, which indicates that the hydrophobic surface formed by Phe-1091 and Phe-1092, Phe-1083 and Leu-1086 is important in the interaction with β 2 TM.

We also note that in lipid bilayers (FTIR experiments) 14 more residues were calculated to be protected from H/D exchange relative to the bicelle system (NMR). This higher number is unlikely to only originate from the inevitably larger error incurred when measuring band areas in IR. Rather, these differences must be of experimental origin; in the NMR experiment, bicelles that have a high curvature are re-solubilized in D_2O . In contrast, in the FTIR experiment, preformed planar lipid bilayers are exposed to D_2O -saturated air. Whether or not the reverse turn is present in the FTIR experiment is not known, but even considering it is present and completely protected from H/D exchange, this is not sufficient to account for these results. We propose that the extra protection to H/D exchange in membranes is due to the formation of a larger proportion of α -helix in extramembrane domains. Indeed, a higher helical content was observed in the FTIR studies performed in membranes (see above), compared to NMR and CD techniques, where bicelles were used. The increased α -helical content in extramembrane regions in supported lipid bilayers relative to the solution NMR conditions may arise

from a far more dehydrated environment in the former. Tight binding of these α -helical domains to the membrane may explain the increased H/D exchange protection. These regions then become unbound, disordered and exposed to solvent when de-reconstituted in bicelles. The above results suggest that data obtained in organic solvents, micelles or bicelles probably underestimates the helical content and membrane binding behavior of juxtamembrane domains, when compared to lipid bilayers. Indeed, in the present work even the reverse turn formed by the GFFKR motif is not totally protected against H/D exchange in bicelles: Phe-1092 is protected, but Gly-1090 and Phe-1091 are not (Fig. 3A), although as discussed above this may arise from experimental protocol differences. In α Ib-TM, both of the equivalent Phe residues, showed little broadening after exposure to Mn^{2+} EDDA2 and H^N - H_2O chemical exchange [17], consistent with some degree of protection. Differences in methodology might also account for the shorter membrane-embedded region for α L, relative to α Ib, determined in the present paper.

Structure of α L in Bicelles

The results of α L structure calculation show that the bicelle-embedded α L peptide adopts a well-defined, highly α -helical conformation at the membrane-spanning region, as expected from a single-pass TM domain. The TM boundaries we found here are generally in agreement with previous studies [17,54,55]. The rest of the α L structure is remarkably similar to α Ib, especially with regards to the two proposed interaction points with the β 2 chain at the two ends of the TM domain, i.e. the OMC and IMC regions.

In the OMC region, both alternative models proposed for α - β heterodimer interaction predict the small residues in the α TM GxxxG-like motif to face the β TM [11], as observed in the α Ib β 3 interface [16]. In α L, a polar residue, Ser-1071, was hypothesized to form a polar interaction with Thr-686 at the binding partner β 2 [36]. Both the alignment of Ser-1071 with Gly-1075 and the hydrophobic IMC region, together with the sensitivity of these residues to titration with the β 2 peptide, are consistent with this part of α L forming a polar interaction with β 2. As polar interactions are stronger in non-polar environments [56,57], this has been proposed to have an impact on integrin deactivation, which is important during leukocyte migration [35]. However, further characterization of the α L/ β 2 interaction is necessary to confirm that point. The OMC region of α L may extend as far as Tyr-1068 and Met-1064, as suggested by the titration experiments.

A chemical shift change was also observed in Asn-1095. This residue was reported to be involved in heterodimerization of the α L β 2 cytoplasmic domain [21]. The equivalent residue in α Ib, Asn-996, experienced a large chemical shift change upon heterodimerization with β 3 TM domain [16]. It is possible that the changes observed in α Ib β 3 Asn-996 are indirectly caused by a nearby salt bridge, Arg-995(α Ib)-Asp723(β 3) [16]. This salt bridge should also be present in α L β 2, between α L Arg-1094 and β 2 Asp-731 [21]. Unfortunately, peak crowding of a large portion of the cytoplasmic tail prevented us from examining the behavior of other residues near this region, e.g. Arg-1094 and Lys-1097.

In summary, we have shown that the conserved GFFKR motif in α integrins forms a structural motif, a backbone reversal, that can be observed when TM domain, cytoplasmic tail and a lipid environment consisting of membranes or bicelles are present, although cytoplasmic tail length may also be an important variable for the stability of this turn [54]. This backbone reversal has been now observed in two different α integrin TMs, α Ib and α L. This is likely to be one of the structural forms of this motif, present in the inactive or intermediate activation state of integrins. We also

show that for α L/ β 2, interaction in the TM domain proper takes place through a remarkably similar structural organization to α IIB/ β 3, with features reminiscent of OMC and IMC clasps. Further studies will include mutagenesis at the predicted α - β interface to confirm the observed interaction, and crucially, determination of interhelical NOE contacts that can unequivocally describe the precise nature of the polar interaction in α L/ β 2 pairs. This work is presently underway.

Supporting Information

File S1 Includes Table S1, Figures S1–S3. Table S1. Structure statistics for the selected 20 structures of integrin α L TM domain. **Figure S1. Expression and purification of integrin α L TM and β 2 TM peptides.** (A) SDS-PAGE of methanol-extracted (meOH) and HPLC-purified (HPLC) α L-TM and β 2-TM peptides. (B) MALDI-TOF MS spectra of the HPLC fractions corresponding to α L TM and β 2 TM peptides. The letters inside square brackets identify the charged species forming a particular peak: M, H, Na, K corresponds to peptide, proton, sodium ion, and potassium ions, respectively. The charge of each species is indicated outside the square bracket. **Figure S2. Secondary structure of the peptide α L used, based on NOE connectivity.** Sequential and medium-ranged NOE connectivity between residues are displayed as bands under the respective residues. The $d_{\alpha N}(i,i+4)$ connectivities indicate the α -helical structure, extending from Leu-1065 to Val-1088. **Figure S3. Secondary structure of integrin TM peptides.** (A) FT-IR spectra of integrin TM α (upper) and β (lower) peptides

reconstituted in DMPC lipid bilayers indicating that both TM peptides are almost completely α -helical. The amide I peak centered at 1657 cm^{-1} (blue) and the Fourier self-deconvolved spectra (red) are shown; (B) CD spectra of integrin TM peptides in DHPC-DMPC bicelles, showing minima at 209 and 222 nm, indicating a high proportion of α -helical form for both peptides; (C) Amide I and amide II regions of integrin TM peptides when bulk water was removed (red) and after D_2O -saturated air exposure (blue). The decrease in the amide II area at $\sim 1550\text{ cm}^{-1}$ indicates H-D exchange. **Figure S4. Effect of increasing concentration on the $[\text{H}^{15}\text{N}]$ -TROSY-HSQC spectrum of α L-TM.** α L TM peptide at 0.1 mM (A) or 0.6 mM (B). α L was reconstituted into DHPC-DMPC bicelles (3% w/v, $q = 0.3$) buffered with 50 mM potassium phosphate at pH 6.5 and spectra were recorded at 305 K. (DOCX)

Acknowledgments

We thank T. Cornvik, A. Oi and E. K.M. Nilsson from NTU/SBS Protein Production Platform for the expression and screening of truncated integrin β 2 TM constructs.

Author Contributions

Conceived and designed the experiments: WS YL OM TD JT. Performed the experiments: WS YL OM TD. Analyzed the data: WS YL. Contributed reagents/materials/analysis tools: OM TD JT. Wrote the paper: WS YL JT.

References

- Hemler M (1999) Extracellular Matrix, Anchor, and Adhesion Proteins; Kreis T, and Vale, R., editor. Oxford: Oxford University Press.
- Carman CV, Springer TA (2003) Integrin avidity regulation: are changes in affinity and conformation underemphasized? *Curr Opin Cell Biol* 15: 547–556.
- Watt FM (2002) Role of integrins in regulating epidermal adhesion, growth and differentiation. *EMBO J* 21: 3919–3926.
- Kim M, Carman CV, Springer TA (2003) Bidirectional transmembrane signaling by cytoplasmic domain separation in integrins. *Science* 301: 1720–1725.
- Hantgan RR, Paumi C, Rocco M, Weisel JW (1999) Effects of ligand-mimetic peptides Arg-Gly-Asp-X (X = Phe, Trp, Ser) on α Ib β 3 integrin conformation and oligomerization. *Biochemistry* 38: 14461–14474.
- Travis MA, Humphries JD, Humphries MJ (2003) An unraveling tale of how integrins are activated from within. *Trends Pharmacol Sci* 24: 192–197.
- Lu CF, Takagi J, Springer TA (2001) Association of the membrane proximal regions of the α and β subunit cytoplasmic domains constrains an integrin in the inactive state. *J Biol Chem* 276: 14642–14648.
- O'Toole TE, Katagiri Y, Faull RJ, Peter K, Tamura R, et al. (1994) Integrin cytoplasmic domains mediate inside-out signal transduction. *J Cell Biol* 124: 1047–1059.
- Lu CF, Springer TA (1997) The alpha subunit cytoplasmic domain regulates the assembly and adhesiveness of integrin lymphocyte function-associated antigen-1. *J Immunol* 159: 268–278.
- Luo BH, Springer TA, Takagi J (2004) A specific interface between integrin transmembrane helices and affinity for ligand. *PLoS Biol* 2: 776–786.
- Gottschalk KE, Adams PD, Brunger AT, Kessler H (2002) Transmembrane signal transduction of the α Ib β 3 integrin. *Protein Sci* 11: 1800–1812.
- MacKenzie KR, Prestegard JH, Engelman DM (1997) A transmembrane helix dimer: Structure and implications. *Science* 276: 131–133.
- Adair BD, Yeager M (2002) Three-dimensional model of the human platelet integrin α Ib β 3 based on electron cryomicroscopy and x-ray crystallography. *Proc Nat Acad Sci USA* 99: 14059–14064.
- Partridge AW, Liu S, Kim S, Bowie JU, Ginsberg MH (2005) Transmembrane domain helix packing stabilizes integrin α Ib β 3 in the low affinity state. *J Biol Chem* 280: 7294–7300.
- Zhu J, Luo BH, Barth P, Schonbrun J, Baker D, et al. (2009) The structure of a receptor with two associating transmembrane domains on the cell surface: integrin α Ib β 3. *Mol Cell* 34: 234–249.
- Lau TL, Kim C, Ginsberg MH, Ulmer TS (2009) The structure of the integrin α Ib β 3 transmembrane complex explains integrin transmembrane signalling. *EMBO J* 28: 1351–1361.
- Lau TL, Dua V, Ulmer TS (2008) Structure of the integrin α Ib transmembrane segment. *J Biol Chem* 283: 16162–16168.
- Chua GL, Patra AT, Tan SM, Bhattacharjya S (2013) NMR Structure of Integrin α 4 Cytosolic Tail and Its Interactions with Paxillin. *PLoS ONE* 8: e55184.
- Chua GL, Tang XY, Patra AT, Tan SM, Bhattacharjya S (2012) Structure and binding interface of the cytosolic tails of α X β 2 integrin. *PLoS ONE* 7: e41924.
- Chua GL, Tang XY, Amalraj M, Tan SM, Bhattacharjya S (2011) Structures and interaction analyses of integrin α M β 2 cytoplasmic tails. *J Biol Chem* 286: 43842–43854.
- Bhunia A, Tang XY, Mohanram H, Tan SM, Bhattacharjya S (2009) NMR solution conformations and interactions of integrin α L β 2 cytoplasmic tails. *J Biol Chem* 284: 3873–3884.
- Vinogradova O, Velyvis A, Velyviene A, Hu B, Haas TA, et al. (2002) A structural mechanism of integrin α (Ib) β (3) “inside-out” activation as regulated by its cytoplasmic face. *Cell* 110: 587–597.
- Vinogradova O, Haas T, Plow EF, Qin J (2000) A structural basis for integrin activation by the cytoplasmic tail of the α (Ib) β -subunit. *Proc Nat Acad Sci USA* 97: 1450–1455.
- Lai C, Liu X, Tian C, Wu F (2013) Integrin α 1 has a long helix, extending from the transmembrane region to the cytoplasmic tail in detergent micelles. *PLoS ONE* 8: e62954. doi:10.1371/journal.pone.0062954.
- Gushiken FC, Patel V, Liu Y, Pradhan S, Bergeron AL, et al. (2008) Protein Phosphatase 2A Negatively Regulates Integrin α Ib β 3 Signaling. *J Biol Chem* 283: 12862–12869.
- Alahari SK, Lee JW, Juliano RL (2000) Nischarin, a Novel Protein That Interacts with the Integrin α 5 Subunit and Inhibits Cell Migration. *J Cell Biol* 151: 1141–1154.
- Alahari SK, Nasrallah H (2004) A membrane proximal region of the integrin α 5 subunit is important for its interaction with nischarin. *Biochem J* 377: 449–457.
- Armulik A, Nilsson I, von Heijne G, Johansson S (1999) Determination of the border between the transmembrane and cytoplasmic domains of human integrin subunits. *J Biol Chem* 274: 37030–37034.
- Naik UP, Patel PM, Parise LV (1997) Identification of a Novel Calcium-binding Protein That Interacts with the Integrin α Ib Cytoplasmic Domain. *J Biol Chem* 272: 4651–4654.
- Tsuboi S (2002) Calcium Integrin-binding Protein Activates Platelet Integrin α Ib β 3. *J Biol Chem* 277: 1919–1923.
- Vallar L, Melchior C, Plançon S, Drobecq H, Lippens G, et al. (1999) Divalent Cations Differentially Regulate Integrin α Ib Cytoplasmic Tail Binding to β 3 and to Calcium- and Integrin-binding Protein. *J Biol Chem* 274: 17257–17266.

32. Rantala JK, Pouwels J, Pellinen T, Veltel S, Laasola P, et al. (2011) SHARPIN is an endogenous inhibitor of [beta]1-integrin activation. *Nat Cell Biol* 13: 1315–1324.
33. Nevo J, Mai A, Tuomi S, Pellinen T, Pentikainen OT, et al. (2010) Mammary-derived growth inhibitor (MDGI) interacts with integrin [alpha]-subunits and suppresses integrin activity and invasion. *Oncogene* 29: 6452–6463.
34. Kinashi T (2007) Integrin regulation of lymphocyte trafficking: lessons from structural and signaling studies. *Adv Immunol* 93: 185–227.
35. Semmrich M, Smith A, Feterowski C, Beer S, Engelhardt B, et al. (2005) Importance of integrin LFA-1 deactivation for the generation of immune responses. *J Exp Med* 201: 1987–1998.
36. Vararattanavech A, Chng CP, Parthasarathy K, Tang XY, Torres J, et al. (2010) A transmembrane polar interaction is involved in the functional regulation of integrin α L β 2. *J Mol Biol* 398: 569–583.
37. Vararattanavech A, Lin X, Torres J, Tan SM (2009) Disruption of the integrin alphaLbeta2 transmembrane domain interface by beta2 Thr-686 mutation activates alphaLbeta2 and promotes micro-clustering of the alphaL subunits. *J Biol Chem* 284: 3239–3249.
38. Chng CP, Tan SM (2011) *Proteins Struct Funct Bioinf* 79: 2203–2213.
39. Sivashanmugam A, Murray V, Cui CX, Zhang YH, Wang JJ, et al. (2009) Practical protocols for production of very high yields of recombinant proteins using *Escherichia coli*. *Protein Sci* 18: 936–948.
40. Studier FW (2005) Protein production by auto-induction in high-density shaking cultures. *Prot Exp Purif* 41: 207–234.
41. Tycko R, Blanco FJ, Ishii Y (2000) Alignment of Biopolymers in Strained Gels: A New Way To Create Detectable Dipole–Dipole Couplings in High-Resolution Biomolecular NMR. *J Am Chem Soc* 122: 9340–9341.
42. Ulmer TS, Ramirez BE, Delaglio F, Bax A (2003) Evaluation of backbone proton positions and dynamics in a small protein by liquid crystal NMR spectroscopy. *J Am Chem Soc* 125: 9179–9191.
43. Dosset P, Hus JC, Marion D, Blackledge M (2001) A novel interactive tool for rigid-body modeling of multi-domain macromolecules using residual dipolar couplings. *J Biomol NMR* 20: 223–231.
44. Cornilescu G, Delaglio F, Bax A (1999) Protein backbone angle restraints from searching a database for chemical shift and sequence homology. *J Biomol NMR* 13: 289–302.
45. Guntert P, Mumenthaler C, Wuthrich K (1997) Torsion angle dynamics for NMR structure calculation with the new program DYANA. *J Mol Biol* 273: 283–298.
46. Herrmann T, Guntert P, Wuthrich K (2002) Protein NMR structure determination with automated NOE assignment using the new software CANDID and the torsion angle dynamics algorithm DYANA. *J Mol Biol* 319: 209–227.
47. Koradi R, Billeter M, Wuthrich K (1996) MOLMOL: a program for display and analysis of macromolecular structures. *J Mol Graph* 14: 51–55, 29–32.
48. Brunger AT (2007) Version 1.2 of the Crystallography and NMR system. *Nat Prot* 2: 2728–2733.
49. Brunger AT, Adams PD, Clore GM, DeLano WL, Gros P, et al. (1998) Crystallography & NMR system: A new software suite for macromolecular structure determination. *Acta Crystallogr, Sect D: Biol Crystallogr* 54: 905–921.
50. Berger BW, Kulp DW, Span LM, DeGrado JL, Billings PC, et al. (2010) Consensus motif for integrin transmembrane helix association. *Proc Nat Acad Sci USA* 107: 703–708.
51. Suk J-E, Situ AJ, Ulmer TS (2012) Construction of Covalent Membrane Protein Complexes and High-Throughput Selection of Membrane Mimics. *J Am Chem Soc* 134: 9030–9033.
52. Vold RR, Prosser RS, Deese AJ (1997) Isotropic solutions of phospholipid bicelles: a new membrane mimetic for high-resolution NMR studies of polypeptides. *J Biomol NMR* 9: 329–335.
53. Li R, Babu CR, Lear JD, Wand AJ, Bennett JS, et al. (2001) Oligomerization of the integrin α Ib β 3: roles of the transmembrane and cytoplasmic domains. *Proc Nat Acad Sci USA* 98: 12462–12467.
54. Yang J, Ma Y-Q, Page RC, Misra S, Plow EF, et al. (2009) *Proc Nat Acad Sci USA* 106: 17729–17734.
55. Armulik A, Nilsson I, von Heijne G, Johansson S (1999) Determination of the border between the transmembrane and cytoplasmic domains of human integrin subunits. *J Biol Chem* 274: 37030–37034.
56. Zhou FX, Merianos HJ, Brunger AT, Engelman DM (2001) Polar residues drive association of polyleucine transmembrane helices. *Proc Nat Acad Sci USA* 98: 2250–2255.
57. Zhou FX, Cocco MJ, Russ WP, Brunger AT, Engelman DM (2000) Interhelical hydrogen bonding drives strong interactions in membrane proteins. *Nat Struct Biol* 7: 154–160.